Octa- and Nonamethylfluorene and an Electron-Rich Permethylfluorenyl Ruthenocene Derivative

Patrick Bazinet, Karl A. Tupper, and T. Don Tilley*

Department of Chemistry, University of California at Berkeley, Berkeley, California 94720-1460, and Chemical Sciences Division, Ernest Orlando Lawrence Berkeley National Laboratory, One Cyclotron Road, Berkeley, California 94720-1460

Received April 18, 2006

Two highly methylated fluorene derivatives have been synthesized and used for the preparation of mixed-ligand fluorenyl ruthenocenes. Specifically, reaction of 2,2′,3,3′,4,4′,5,5′-octamethylbiphenyl with paraformaldehyde in the presence of CF_3CO_2H provided 1,2,3,4,5,6,7,8-octamethylfluorene ($C_{13}Me_8H_2$), which was subsequently methylated by reaction with *n*-BuLi followed by addition of MeI to yield 1,2,3,4,5,6,7,8,9-nonamethylfluorene ($C_{13}Me_9H$). Reaction of the lithium fluorenyl derivatives with $[Cp^*RuCl]_4$ generated the mixed-ligand ruthenocenes $Cp^*(C_{13}Me_8H)Ru$ and $Cp^*(C_{13}Me_9)Ru$. Electrochemical measurements indicate that these ruthenocene derivatives undergo quasi-reversible oxidations at low potentials consistent with strongly donating character for the highly methylated fluorenyl ligands. X-ray diffraction studies on $C_{13}Me_8H_2$, $C_{13}Me_9H$, and $Cp^*(C_{13}Me_9)Ru$ revealed a twisted fluorene core in all cases.

Introduction

The cyclopentadienyl ligand (Cp, C_5H_5) and its derivatives have played a prominent role in the development of organometallic chemistry and catalysis. These robust and versatile ligands strongly influence the chemistry of their complexes; therefore, considerable attention has been devoted to manipulation of the structural and electronic modifications of Cp-type structures. In particular, methylated Cp derivatives have provided many key advances in transition-metal chemistry,[1] and the permethylated analogue (Cp*, C_5Me_5) has been established as a highly sterically demanding, electron-donating ligand. Thus, Cp* has been extensively used in the development of main-group-, early transition-, and f-metal chemistry, where it serves to stabilize reactive, monomeric forms of coordinatively unsaturated complexes.[2,3] Another important modification to the basic Cp ligand structure involves incorporation of a fused aromatic ring (Chart 1). Such ligands, with their extended π systems, exhibit novel electronic and dynamic properties. The indenyl ligand (Ind, C_9H_7) has attracted considerable attention in this regard, and it is well known for its ability to enhance the reactivity of its complexes via low-energy changes in its coordination mode, from η^5 to η^3 (the "indenyl effect").[4] Although used less frequently than Cp or Ind derivatives, the fluorenyl ligand (Flu, $C_{13}H_9$) exhibits a high donor ability and varied coordination modes.[5,6]

Chart 1

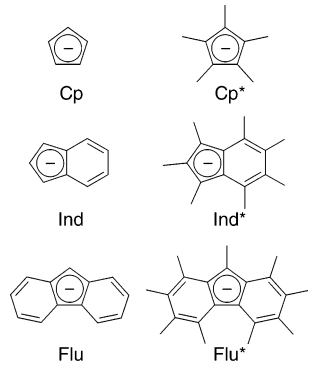

The permethylated indenyl ligand[7] (Ind*, C_9Me_7) represents a rarely employed but potentially useful ligand featuring strong electron donation and the possibility for facile changes in

* To whom correspondence should be addressed. Tel: 510 642 8939. Fax: 510 642 8940. E-mail: tdtilley@berkeley.edu.

(1) For reviews on the application of highly substituted cyclopentadienyl ligands, see: (a) Janiak, C.; Schumann, H. *Adv. Organomet. Chem.* **1991**, *33*, 291. (b) Okuda, J. *Top. Curr. Chem.* **1991**, *160*, 97.

(2) For example, Cp* has been used to stabilize the following. (a) $[Cp^*_2Ti]$: Bercaw, J. E.; Marvich, R. H.; Bell, L. G.; Brintzinger, H. H. *J. Am. Chem. Soc.* **1972**, *94*, 1219. (b) $[Cp^*_2Zr(N_2)]_2N_2$: Manriquez, J. M.; Bercaw, J. E. *J. Am. Chem. Soc.* **1974**, *96*, 6229. (c) $Cp^*_2M(CH_3)_2$ (M = U, Th): Manriquez, J. M.; Fagan, P. J.; Marks, T. J. *J. Am. Chem. Soc.* **1978**, *100*, 3939. (d) $[Cp^*_2Ta(H){=}CH_2]$: van Asselt, A.; Burger, B. J.; Gibson, V. C.; Bercaw, J. E. *J. Am. Chem. Soc.* **1986**, *108*, 5347. (e) Cp^*_2Ln (Ln = Sm): Evans, W. J.; Hughes, L. A.; Hanusa, T. P. *J. Am. Chem. Soc.* **1984**, *106*, 4270. (f) Cp^*_2Ln (Ln = Eu, Yb): Andersen, R. A.; Boncella, J. M.; Burns, C. J.; Green, J. C.; Hohl, D.; Rösch, N. *J. Chem. Soc., Chem. Commun.* **1986**, 405. (g) Cp*ZnZnCp*: Resa, I.; Carmona, E.; Gutierrez-Puebla, E.; Monge, A. *Science* **2004**, *305*, 1136.

(3) For a recent review on Cp* main-group chemistry, see: Jutzi, P.; Reumann, G. *J. Chem. Soc., Dalton Trans.* **2000**, 2237.

(4) (a) Rerek, M. E.; Ji, L.-N.; Basolo, F. *J. Chem. Soc., Chem. Commun.* **1983**, 1208. (b) O'Connor, J. M.; Casey, C. P. *Chem. Rev.* **1987**, *87*, 307. (c) Westcott, S. A.; Kakkar, A. K.; Stringer, G.; Taylor, N. J.; Marder, T. B. *J. Organomet. Chem.* **1990**, *394*, 777. (d) Calhorda, M. J.; Veiros, L. F. *J. Organomet. Chem.* **2001**, *635*, 197. (e) Calhorda, M. J.; Romão, C. C.; Veiros, L. F. *Chem. Eur. J.* **2002**, *8*, 868. (f) For a review on indenyl complexes of group 8 metals see: Cadierno, V.; Díez, J.; Gamasa, M. P.; Gimeno, J.; Lastra, E. *Coord. Chem. Rev.* **1999**, *193*−*195*, 147. (g) For a review on indenyl complexes of group 10 metals see: Zargarian, D. *Coord. Chem. Rev.* **2002**, *233*−*234*, 157.

(5) For reviews on early-transition-metal fluorenyl compounds see: (a) Kirillov, E.; Saillard, J.-Y.; Carpentier, J.-F. *Coord. Chem. Rev.* **2005**, *249*, 1221. (b) Alt, H. G.; Samuel, E. *Chem. Soc. Rev.* **1998**, *27*, 323.

(6) Examples of late-transition-metal fluorenyl complexes exhibiting varied coordination modes include: (a) Young, K. M.; Miller, T. M.; Wrighton, M. S. *J. Am. Chem. Soc.* **1990**, *112*, 1529. (b) Ji, L.-N.; Rerek, M. E.; Basolo, F. *Organometallics* **1984**, *3*, 740. (c) Treichel, P. M.; Fivizzani, K. P.; Haller, K. J. *Organometallics* **1982**, *1*, 931. (d) Treichel, P. M.; Johnson, J. W. *Inorg. Chem.* **1977**, *16*, 749. (e) Johnson, J. W.; Treichel, P. M. *J. Chem. Soc., Chem. Commun.* **1976**, 688.

(7) Miyamoto, T. K.; Tsutsui, M.; Chen, L.-B. *Chem. Lett.* **1981**, 729.

10.1021/om0603464 CCC: $33.50
Publication on Web 07/28/2006

Scheme 1

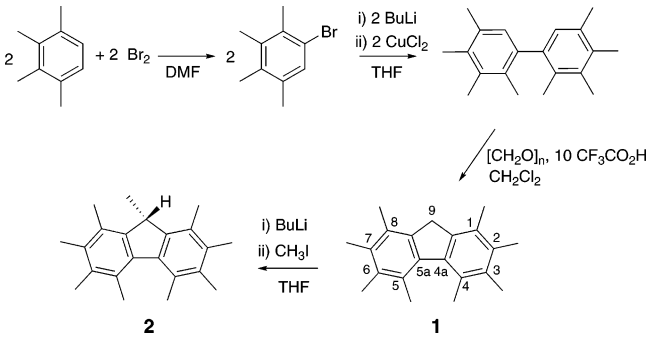

coordination modes.[8] Comparisons of electronic properties of 16- and 18-electron chromium and iron metallocenes containing Cp* or Ind* ligands suggest that Ind* is more electron-donating, on the basis of electrochemical oxidation potentials and ionization energies. However, in the case of the 19-electron cobaltocene derivatives, the Ind* ligand appears less donating.[9] These results raise interesting questions regarding the potential properties of the heretofore unknown permethylated fluorenyl ligand (Flu*, $C_{13}Me_9$). In this contribution, we report the synthesis of 1,2,3,4,5,6,7,8,-octamethylfluorene and 1,2,3,4,5,6,7,8,9-nonamethylfluorene and their use in the preparation of mixed-ligand ruthenocenes. We also describe single-crystal X-ray diffraction and electrochemical studies that clearly demonstrate the unusual properties of these electron-rich ligands.

Results and Discussion

Synthesis and Characterization of Methylated Fluorene Derivatives. The desired permethylated ligand precursor was synthesized in four steps from 1,2,3,4-tetramethylbenzene (Scheme 1). Using a modified[10] procedure, 2,3,4,5-tetramethylbromobenzene was obtained by bromination with Br_2 in dimethylformamide. Only 1 equiv of bromine is used to prevent formation of any dibrominated product. The resulting moderate yield of approximately 50% is compensated by the easy recovery of any unreacted starting material via distillation. Homocoupling of the aryl bromide to generate the known 2,2′,3,3′,4,4′,5,5′-octamethylbiphenyl[11] in yields ranging from 40 to 65% was achieved via lithiation, using *n*-BuLi, followed by addition of $CuCl_2$. Transformation of the biphenyl into a fluorene derivative was accomplished through an electrophilic aromatic substitution and cyclization, using paraformaldehyde and trifluoroacetic acid. This reaction generated 1,2,3,4,5,6,7,8-octamethylfluorene (**1**) in moderate yields ranging from 35 to 60%. The final methylation step was accomplished by deprotonation of **1** followed by addition of iodomethane and provided the desired 1,2,3,4,5,6,7,8,9-nonamethylfluorene (**2**) in high yields (87−96%).

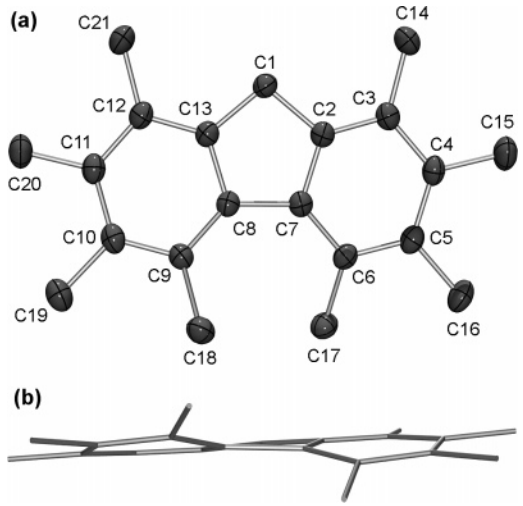

Figure 1. Thermal ellipsoid plot (a) and stick diagram (b) for compound **1**. Hydrogen atoms are omitted for clarity. Thermal ellipsoids are drawn at 50% probability. The C(6)−C(7)−C(8)−C(9) dihedral angle is 21.0(2)°.

The ^{1}H NMR spectrum for compound **1** exhibits a singlet for the methylene protons at 3.70 ppm along with three other singlets at 2.43, 2.35, and 2.30 ppm integrating for six, six, and 12 protons, respectively, and suggests a symmetric structure with four distinct methyl groups, two of which have overlapping signals in the spectrum. The ^{13}C{^{1}H} NMR spectrum reveals four signals for the methyl group carbons, one signal for the methylene carbon, and six signals for the aromatic carbons forming the six-membered rings of the fluorene.

Compound **2** displays spectroscopic characteristics similar to those of **1**, with a few differences arising from the presence of the additional methyl group. In the ^{1}H NMR spectrum, the unique methyl group at the 9-position appears as a doublet (1.35 ppm) due to coupling with the methine proton, which in turn appears as a quartet (3.99 ppm). The other methyl groups give rise to four distinct singlets between 2.35 and 2.16 ppm. As expected, the ^{13}C{^{1}H} NMR spectrum clearly displays five signals for the methyl carbons, one for the tertiary carbon, and six peaks in the aromatic region.

Molecular structures of **1** and **2**, obtained from the single-crystal X-ray analyses, are illustrated in Figures 1 and 2. The most salient feature of these molecular structures is the substantial distortion from planarity of the fluorene ring skeleton. The apparent reason for the severe twisting of the normally planar fluorene structure is the steric repulsion between the two methyl substituents at the 4- and 5-positions. The distances between the carbon atoms of these methyl groups at 3.07 and 3.08 Å for compounds **1** and **2**, respectively, are significantly smaller than the sum of the van der Waals radii of two methyl groups (4.0 Å). The amount of twist can be measured by the dihedral angle formed by the four carbons at the 4-, 4a-, 5a-, and 5-positions of the fluorene. The measured dihedral angles for compounds **1** and **2** of 21.0(2)° and 22.7(6)°, respectively, are in line with those of other twisted fluorene derivatives such as 1,2,3,4,5,6,7,8-octaethylfluorene (29.6°) and 2,3,5,6,7,8,9-heptaphenyl-1,4-di(*p*-tolyl)fluorene (19.3°).[12] This twist causes the methyl substituents to be pushed toward opposite sides of

(8) For examples see: (a) Rerek, M. E.; Basolo, F. *J. Am. Chem. Soc.* **1984**, *106*, 5908. (b) Kakkar, A. K.; Jones, S. F.; Taylor, N. J.; Collins, S.; Marder, T. B. *J. Chem. Soc., Chem. Commun.* **1989**, 1454. (c) Kakkar, A. K.; Taylor, N. J.; Marder, T. B.; Shen, J. K.; Hallinan, N.; Basolo, F. *Inorg. Chim. Acta* **1992**, *198*−*200*, 219. (d) Kakkar, A. K.; Stringer, G.; Taylor, N. J.; Marder, T. B. *Can. J. Chem.* **1995**, *73*, 981. (e) Mantovani, L.; Ceccon, A.; Gambaro, A.; Santi, S.; Ganis, P.; Venzo, A. *Organometallics* **1997**, *16*, 2682. (f) Haynes, A.; Haslam, C. E.; Bonnington, K. J.; Parish, L.; Adams, H.; Spey, S. E.; Marder, T. B.; Coventry, D. N. *Organometallics* **2004**, *23*, 5907. (g) Gavenonis, J.; Tilley, T. D. *J. Organomet. Chem.* **2004**, *689*, 870.

(9) (a) O'Hare, D.; Green, J. C.; Marder, T.; Collins, S.; Stringer, G.; Kakkar, A. K.; Kaltsoyannis, N.; Kuhn, A.; Lewis, R.; Mehnert, C.; Scott, P.; Kurmoo, M.; Pugh, S. *Organometallics* **1992**, *11*, 48. (b) O'Hare, D.; Murphy, V. J.; Kaltsoyannis, N. *J. Chem. Soc., Dalton Trans.* **1993**, 383.

(10) Smith, L. I.; Moyle, C. L. *J. Am. Chem. Soc.* **1933**, *55*, 1676.

(11) (a) de la Mare, P. B. D.; Johnson, E. A.; Lomas, J. S. *J. Chem. Soc.* **1965**, 6893. (b) Hart, H.; Teuerstein, A. *Synthesis* **1979**, *9*, 693.

(12) (a) Marks, V.; Gottlieb, H. E.; Melman, A.; Byk, G.; Cohen, S.; Biali, S. E. *J. Org. Chem.* **2001**, *66*, 6711. (b) Tong, L.; Lau, H.; Ho, D. M.; Pascal, R. A., Jr. *J. Am. Chem. Soc.* **1998**, *120*, 6000. (c) Nishinaga, T.; Inoue, R.; Matsuura, A.; Komatsu, K. *Org. Lett.* **2002**, *4*, 4117. (d) Eichler, B. E.; Miracle, G. E.; Powell, D. R.; West, R. *Main Group Met. Chem.* **1999**, *22*, 147.

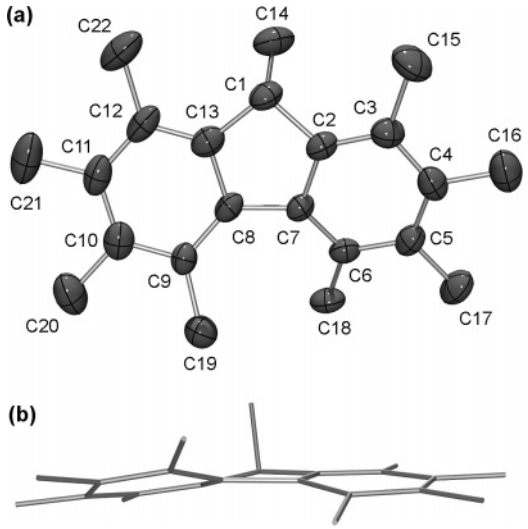

Figure 2. Thermal ellipsoid plot (a) and stick diagram (b) for compound **2**. Hydrogen atoms are omitted for clarity. Thermal ellipsoids are drawn at 50% probability. The C(6)−C(7)−C(8)−C(9) dihedral angle is 22.7(6)°.

the fluorene plane, and for the octamethylfluorene **1**, this generates a C_2 symmetric species. However, the presence of the additional methyl substituent in nonamethylfluorene **2** breaks this symmetry and renders all eight arene methyl groups unique. The fact that the NMR spectra for **2** exhibit only five signals for the methyl groups indicates that this twisted structure is fluxional in solution.

Synthesis and Characterization of Mixed-Ligand Ruthenocenes. The synthesis of highly methylated fluorenes was undertaken with the idea of creating new Cp-type ligands with sterically demanding and strongly donating properties. The synthesis and characterization of 18-electron metallocene derivatives was envisioned as a simple, initial way to evaluate the inherent properties of the new fluorenyl ligands. Therefore, we chose to prepare mixed-ligand ruthenocenes containing one Cp* ligand and either the octa- or nonamethylfluorenyl ligand.[13,14] Deprotonation of **1** and **2** with an alkyllithium base, followed by addition of the half-sandwich compound $[Cp^*RuCl]_4$, yielded the desired metallocenes $Cp^*(C_{13}Me_8H)Ru$ (**3**) and $Cp^*(C_{13}Me_9)Ru$ (**4**) in moderate yields (eq 1). Spectroscopic characterizations of these products are consistent with the expected metallocene structures.

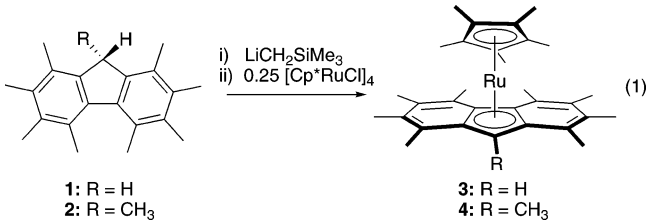

The ^{1}H NMR spectrum of compound **3** displays a total of five singlets in a 1:6:6:12:15 ratio. The anionic nature of the ligand is confirmed by a peak at 5.18 ppm (1H), which is assigned to the newly generated aromatic proton. Just as for compound **1**, the ^{1}H NMR spectrum reveals only three signals for the four methyl groups of the $C_{13}Me_8H$ ligand due to two overlapping peaks. For **3**, metal coordination of the $C_{13}Me_8H$ ligand renders one face unique, thereby breaking the C_2 symmetry and making all eight methyl substituents inequivalent; however, the $^{13}C\{^1H\}$ NMR spectrum displays only four signals for the methyl groups of the $C_{13}Me_8H$ ligand. These results imply either that the twisted ligand core undergoes rapid interconversion or that the ligand adopts a planar geometry upon metal coordination.

(13) The related Cp*(Flu)Ru has been reported in: (a) Gassman, P. G.; Winter, C. H. *J. Am. Chem. Soc.* **1988**, *110*, 6130. (b) Kudinov, A. R.; Shul'pina, L. S.; Petrovskii, P. V.; Rybinskaya, M. I. *Metalloorg. Khim.* **1990**, *3*, 1391.

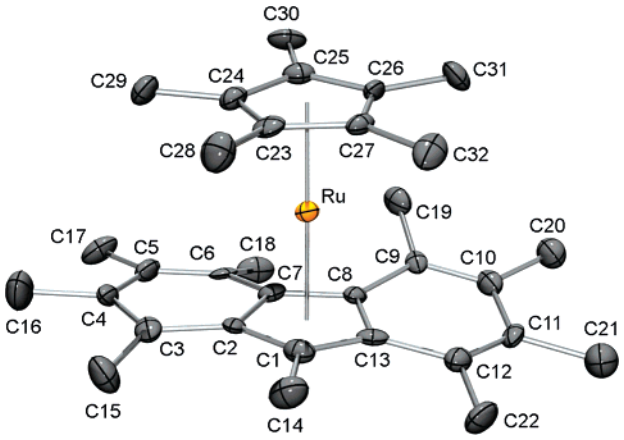

Figure 3. Thermal ellipsoid plot for compound **4**. Hydrogen atoms have been omitted for clarity. Thermal ellipsoids are drawn at 50% probability.

Table 1. Selected Bond Distances and Angles for 4

	Distances (Å)		
Ru−C(1)	2.188(6)	Ru−C(23)	2.170(6)
Ru−C(2)	2.218(11)	Ru−C(24)	2.150(6)
Ru−C(7)	2.251(6)	Ru−C(25)	2.211(7)
Ru−C(8)	2.212(6)	Ru−C(26)	2.172(10)
Ru−C(13)	2.263(7)	Ru−C(27)	2.153(6)
Flu^*_{cent}−Ru	1.85(3)	Cp^*_{cent}−Ru	1.80(3)
	Angles (deg)		
C(6)−C(7)−C(8)−C(9)	16(1)	Cp^*_{cent}−Ru−Flu^*_{cent}	179.2(7)

The NMR spectra of compound **4** exhibit characteristics similar to those of **3**. The fact that the nine methyl groups of the Flu* ligand appear as only five signals in the ^{1}H NMR spectrum once again suggests that the ligand assumes a planar geometry upon coordination to Ru or that the twisted structure rapidly interconverts between the two rotamers. The $^{13}C\{^1H\}$ NMR spectrum of compound **4** is consistent with the ^{1}H NMR spectrum and displays five signals for the methyl groups of the Flu* ligand and seven signals for the fluorene core. Low-temperature ^{1}H NMR spectra (−40 to −80 °C) of compound **4** exhibited only five signals for the methyl groups of the Flu* ligand, suggesting a very low energy barrier for any fluxional process.

The molecular structure of **4**, determined by X-ray crystallography, is illustrated in Figure 3. Selected bond lengths and angles are listed in Table 1. The solid-state structure of compound **4** is, in essence, similar to that of a typical metallocene and resembles that previously reported for Cp*(Flu)Ru.[13a,15] The two Cp-type ligands exhibit η^5-coordination to the Ru center

(14) Examples of other ruthenium fluorenyl compounds include: (a) Buchmeiser, M.; Schottenberger, H. *Organometallics* **1993**, *12*, 2472. (b) Wheeler, D. E.; Bitterwolf, T. E. *Inorg. Chim. Acta* **1993**, *205*, 123. (c) Yang, J.; Jones, W. M.; Dixon, J. K.; Allison, N. T. *J. Am. Chem. Soc.* **1995**, *117*, 9776. (d) Lau, C. S.-W.; Wong, W.-T. *J. Chem. Soc., Dalton Trans.* **1999**, 607. (e) Sun, Y.; Chan, H.-S.; Dixneuf, P. H.; Xie, Z. *Organometallics* **2004**, *23*, 5864.

(15) The structure of the related compound Cp*(Flu)Os was reported in: Arachchige, S. M.; Heeg, M. J.; Winter, C. H. *J. Organomet. Chem.* **2005**, *690*, 4356.

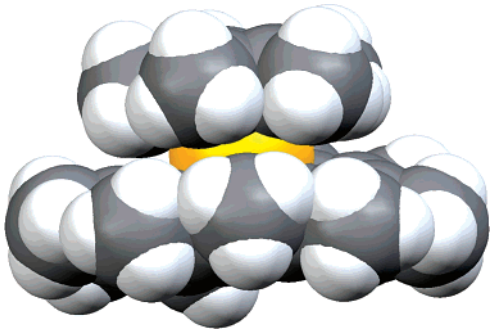

Figure 4. Space-filling diagram of compound **4**.

with a staggered conformation and are essentially parallel to each other, with a dihedral angle of 3.0° between the mean planes of the five-membered rings and a centroid−Ru−centroid angle of 179.2(7)°. However, the molecular structure reveals a Flu* ligand that is significantly distorted from planarity due to steric repulsions between methyl groups, which results in a twist of the fluorene core. The distance between the carbon atoms of the methyl groups of 3.03 Å is similar to the corresponding values obtained for compounds **1** and **2**. Interestingly, the C(6)−C(7)−C(8)−C(9) dihedral angle of 16(1)° is significantly smaller than the analogous angle in the parent compound **2**. Though many factors probably contribute to this reduction in the torsion angle, coordination of the Cp*Ru fragment undoubtedly imposes a steric compression of the ligand.

Previous work with mixed-ligand ruthenocenes containing Cp, Cp*, Ind, and Flu ligands revealed a trend whereby the metal center lies closest to the least electron-donating ligand.[13a] Although the two Ru−centroid distances in compound **4** differ, with the Ru−Cp*$_{centroid}$ length being shorter (1.80(3) Å) than the Ru−Flu*$_{centroid}$ distance (1.85(3) Å), the large errors in the calculated distances make any conclusions impossible. The Ru−carbon distances involving the Cp* ring are essentially the same (av 2.17 Å); however, the corresponding distances to the central ring carbons of the Flu* ligand range from 2.188(6) to 2.263(7) Å. For fluorenyl compounds the metal is typically closest to the carbon at the 9-position, and although this is true in compound **4**, the twist in the fluorene core causes significant variations in the Ru−carbon distances, resulting in one short (2.188(6) Å), two intermediate (2.212(6) and 2.218(11) Å), and two long (2.251(6) and 2.263(7) Å) distances. Most likely, these variations result from the twisted ligand structure rather than a "slippage" of the ligand to another coordination mode. In addition to providing critical bonding parameters, the molecular structure of compound **4** illustrates the unique structural features of the Flu* ligand. The very large size of the ligand becomes apparent upon inspection of a space-filling diagram of compound **4** (Figure 4), which displays the Flu* ligand occupying approximately one-half of the metal's coordination sphere.

Electrochemical Measurements. The electronic properties of mixed-ligand ruthenocene derivatives have been examined by electrochemical and XPS studies.[13a,16] On the basis of oxidation potentials and XPS binding energies, it was proposed that the fluorenyl (Flu) ligand is more electron-donating than Cp*. However, free energies of ionization, determined by gas-phase electron-transfer equilibrium measurements, indicated that the Flu ligand is less donating, and the discrepancy between these results was attributed to inaccuracy of oxidation potentials due to irreversible oxidations and differences in solvation energies between metal complexes.[17]

To gain an understanding of the influence methylation has on the electronic properties of the fluorenyl ligand, electrochemical measurements were performed on the ruthenocene derivatives **3** and **4**, as well as decamethylruthenocene (**5**) for comparison. The measurements were performed in dichloromethane containing 0.1 M tetra-*n*-butylammonium perchlorate ($TBA^+ClO_4^-$) as supporting electrolyte, and the observed oxidation potentials were referenced to an external ferrocene standard. Table 2 lists the electrochemical oxidation potentials ($E^{\circ\prime}$) of **3**, **4**, and **5**, as determined by cyclic voltammetry. Table 2 also contains reported $E^{\circ\prime}$ values for other pertinent analogues. For both **3** and **4**, quasi-reversible oxidations, indicated by current ratios and peak-to-peak separations, were observed. Interestingly, when the scanning ranges were widened, both compounds exhibited an additional irreversible oxidation peak, which presumably results from the generation of Ru^{IV} dications.[18] The considerably lower $E^{\circ\prime}$ values for **3** and **4** (0.22 and 0.16 V, respectively) compared to those of Cp*$_2$Ru (0.56 V) and Cp*(Flu)Ru (0.51 V) suggest that the methylated fluorenyl ligands are significantly more electron-donating than the Cp* and Flu ligands. Table 2 also includes reported electrochemical data obtained using the large noncoordinating tetra-*n*-butylammonium tetra[3,5-bis(trifluoromethyl)phenyl]borate (TBA^+TFPB^-) as an electrolyte to enhance the reversibility of redox couples.[16,19] Although it is difficult to compare results obtained under different conditions, the reported $E^{\circ\prime}$ values exhibit the same trend in ligand electron-donating properties.

Concluding Remarks

With the goal of expanding the number of strongly donating, sterically demanding Cp-type ligands, the preparations of octa- and nonamethylfluorene were carried out. Molecular structures of the highly substituted fluorenes display severely distorted fluorene cores in the solid state. Mixed-ligand ruthenocenes containing these ligands were prepared by reaction of the lithium fluorenyl derivatives with [Cp*RuCl]$_4$. Structural characterization of the first metal complex containing the permethylated fluorenyl ligand, Cp*(Flu*)Ru, revealed Flu* to be η^5-coordinated to the metal center. The molecular structure also demonstrates the severely twisted and very expansive nature of the ligand. Electrochemical measurements performed on the novel ruthenocene derivatives indicate that these heavily methylated fluorenyl ligands are more electron-donating than Flu and Cp*. Continuing work is focused on exploration of the coordination chemistry of these new ligands with early- and late-transition metals, as well as further investigations into their inherent structural and electronic properties and how these might affect metal-centered chemistry and catalysis.

Experimental Section

General Comments. All air-sensitive manipulations were performed under an atmosphere of nitrogen using Schlenk techniques and/or a Vacuum Atmospheres glovebox. Dry, oxygen-free solvents were employed for all air-sensitive manipulations. Removal of thiophenes from benzene and toluene was accomplished by washing each with H_2SO_4 and saturated $NaHCO_3$ followed by drying over

(16) Gassman, P. G.; Sowa, J. R., Jr.; Hill, M. G.; Mann, K. R. *Organometallics* **1995**, *14*, 4879.

(17) Ryan, M. F.; Siedle, A. R.; Burk, M. J.; Richardson, D. E. *Organometallics* **1992**, *11*, 4231.

(18) Related group 8 *ansa*-metallocene dications have been isolated for Ru: (a) Hashidzume, K.; Tobita, H.; Ogino, H. *Organometallics* **1995**, *14*, 1187. And for Fe: (b) Ogino, H.; Tobita, H.; Habazaki, H.; Shimoi, M. *J. Chem. Soc., Chem. Commun.* **1989**, 828.

(19) Hill, M. G.; Lamanna, W. M.; Mann, K. R. *Inorg. Chem.* **1991**, *30*, 4687.

Table 2. Electrochemical Data for Various Ruthenocene Derivatives

	$TBA^+ClO_4^-/CH_2Cl_2$			TBA^+TFPB^-/CH_2Cl_2		
compound	$E^{o\prime}$ (V)[a]	ΔE (V)[a,b]	$i_{p,c}/i_{p,a}$[a,c]	$E^{o\prime}$ (V)[e]	ΔE (V)[e]	$i_{p,c}/i_{p,a}$[e]
Cp_2Ru	0.97[d]		0.60[d]	1.03	0.089	0.94
Cp*(Cp)Ru	0.71[d]		0.55[d]	0.69	0.099	0.81
Cp*(Ind)Ru	0.60[d]		0.68[d]	0.51	0.084	1.0
Cp^*_2Ru (**5**)	0.56	0.147	0.99	0.48	0.080	1.0
Cp*(Flu)Ru	0.51[d]		0.38[d]	0.41	0.096	0.88
$Cp^*(C_{13}Me_8H)Ru$ (**3**)	0.22	0.112	0.69			
$Cp^*(C_{13}Me_9)Ru$ (**4**)	0.16	0.126	0.92			

[a] Potentials ($E^{o\prime}$) vs $Ag/AgNO_3$ in a 0.10 M $TBA^+ClO_4^-/CH_3CN$ solution calibrated using an $E^{o\prime}$ value of ferrocene of 0.47 V. The scan rate was 100 mM s^{-1}. The electrolyte/solvent system is 0.10 M $TBA^+ClO_4^-/CH_2Cl_2$, and ca. 0.5−1.0 mM solutions of the complexes were used. [b] Anodic potential ($E_{p,a}$) minus cathodic potential ($E_{p,c}$) determined by CV. [c] Ratio of cathodic current ($i_{p,c}$) to anodic current ($i_{p,a}$). [d] Reference 13a. Potentials ($E_{1/2}$) vs SCE were calculated using an $E^{o\prime}$ value for ferrocene of 0.48 V (see ref 16). [e] Reference 16. Potentials ($E^{o\prime}$) vs aqueous Ag/AgCl in 1.0 M KCl using an $E^{o\prime}$ value of ferrocene of 0.47 V. The electrolyte/solvent system is 0.10 M TBA^+TFPB^-/CH_2Cl_2.

$MgSO_4$. All dried solvents were distilled from sodium benzophenone ketyl, with the exception of benzene-d_6, which was purified by vacuum distillation from Na/K alloy, and dichloromethane-d_2, which was purified by vacuum distillation from CaH_2. The compounds $LiCH_2SiMe_3$,[20] Cp^*_2Ru,[21] and $[Cp^*RuCl]_4$[22] were prepared according to literature procedures. Other chemicals were purchased, 1,2,3,4-tetramethylbenzene (TCI America or Alfa Aesar), Br_2, $CuCl_2$, BuLi (1.6 M in hexane), paraformaldehyde, CF_3CO_2H, CH_3I (Aldrich), $MgSO_4$, Na_2SO_3 (EMD Chemicals), and used as received. Elemental analyses were performed by the microanalytical laboratory at the University of California, Berkeley. All NMR spectra were recorded at room temperature unless otherwise noted, using either a Bruker AM-400, AMX-400, or AMX-300 instrument.

2,3,4,5-Tetramethylbromobenzene.[10] A 500 mL round-bottom flask wrapped in aluminum foil was charged with tetramethylbenzene (19.83 g, 0.148 mol) and dimethylformamide (100 mL) and cooled to 0 °C. A solution of bromine (23.7 g, 0.148 mmol) in DMF (30 mL) was cooled to 0 °C and added dropwise to the reaction flask. The reaction mixture was allowed to warm to room temperature and was then stirred for 20 h. An aqueous Na_2SO_3 solution was slowly added to the reaction (use of an ice bath is recommended for large-scale reactions) until the orange bromine color disappeared (ca. 0.5 equiv). Hexanes were added (100 mL), and the phases were separated. The aqueous phase was washed with hexanes (2 × 50 mL), and all the organic extracts were combined, dried with $MgSO_4$, and concentrated under vacuum. Vacuum distillation with the distillate flask cooled to 0 °C allowed for separation of the starting material (20−50 °C, 40 mmHg, 9.31 g, 47%) from the desired product (51−53 °C, 40 mmHg, 15.14 g, 48%), which slowly solidified in the chilled distillate flask. ^1H NMR (chloroform-*d*, 300 MHz, 25 °C): δ 7.27 (s, 1H, Ar-*H*), 2.41 (s, 3H, C*H*$_3$), 2.28 (s, 3H, C*H*$_3$), 2.26 (s, 3H, C*H*$_3$), 2.17 (s, 3H, C*H*$_3$).

2,2′,3,3′,4,4′,5,5′-Octamethylbiphenyl.[11] A 250 mL Schlenk flask was charged with 2,3,4,5-tetramethylbromobenzene (12.7 g, 59.6 mmol) and THF (100 mL) and cooled to −78 °C. Upon slow addition of a *n*-BuLi solution (41 mL, 1.6 M in hexanes, 65.6 mmol), a white precipitate formed, and the mixture was stirred for 1 h at −78 °C. Solid $CuCl_2$ (8.82 g, 65.6 mmol) was added, and the reaction mixture was stirred for 20 min at −78 °C, then allowed to slowly warm to room temperature and stirred for an additional 20 h. The reaction mixture was exposed to air and stirred for 30 min. Approximately 25 mL of a 2 M HCl solution was added, and the mixture was stirred for 15 min. Hexanes (50 mL) and water (50 mL) were added, and the layers were separated. The aqueous layer was subsequently washed with hexanes (50 mL) and dichloromethane (50 mL). The organic extracts were combined, dried with $MgSO_4$, and filtered. All volatile materials were removed under vacuum to leave a pasty yellow solid. Purification by column chromatography (SiO_2, 9:1 hexanes/CH_2Cl_2) yielded the pure product as a white solid (5.1 g, 64%). ^1H NMR (chloroform-*d*, 300 MHz, 25 °C): δ 6.82 (s, 2H, Ar-*H*), 2.29 (s, 6H, C*H*$_3$), 2.274 (s, 6H, C*H*$_3$), 2.266 (s, 6H, C*H*$_3$), 2.00 (s, 6H, C*H*$_3$).

1,2,3,4,5,6,7,8-Octamethylfluorene (1). A 250 mL Schlenk flask was charged with octamethylbiphenyl (2.58 g, 9.69 mmol) and paraformaldehyde (0.364 g, 12.1 mmol). Approximately 100 mL of CH_2Cl_2 was cannula-transferred into the flask, and trifluoroacetic acid (7.5 mL) was added to this suspension, dropwise via syringe. As the acid was being added, a pink color started to appear, and all solids dissolved. The reaction was stirred for 18 h and turned to a dark burgundy red. The reaction was slowly poured into a mixture of water (100 mL) and CH_2Cl_2 (100 mL). Aqueous NaOH was carefully added until a pH of 10 was reached. The layers were separated, and the aqueous layer was washed with CH_2Cl_2 (2 × 50 mL). The organic extracts were combined, dried with $MgSO_4$, and filtered. All volatile materials were removed under vacuum to leave a sticky brown solid, which was washed with small amounts of hexanes (2 × 5 mL) to remove impurities. The product was obtained as a beige solid with a purity of ca. 95% (1.42 g, 53%). The product can be further purified by crystallization from hot toluene. X-ray-quality crystals were obtained by slow evaporation of a toluene solution of **1**. ^1H NMR (chloroform-*d*, 400 MHz, 25 °C): δ 3.70 (s, 2H, C*H*$_2$), 2.43 (s, 6H, C*H*$_3$), 2.35 (s, 6H, C*H*$_3$), 2.30 (s, 12H, C*H*$_3$). $^{13}C\{^1H\}$ NMR (chloroform-*d*, 100 MHz, 25 °C): δ 140.0 (2C, *C*), 139.9 (2C, *C*), 134.4 (2C, *C*), 132.8 (2C, *C*), 128.9 (2C, *C*), 127.8 (2C, *C*), 36.7 (1C, *C*H$_2$), 21.7 (2C, *C*H$_3$), 16.5 (2C, *C*H$_3$), 16.3 (2C, *C*H$_3$), 16.1 (2C, *C*H$_3$). Anal. Calcd for $C_{21}H_{26}$: C, 90.59; H, 9.41. Found: C, 90.68; H, 9.53.

1,2,3,4,5,6,7,8,9-Nonamethylfluorene (2). A 500 mL flask was charged with compound **1** (2.10 g, 7.55 mmol) and THF (200 mL), and the resulting solution was cooled to 0 °C. Upon slow addition of a *n*-BuLi solution (5.43 mL, 1.6 M hexanes, 8.69 mmol), a dark red color appeared, and the reaction mixture was stirred for 1.5 h at 0 °C. Addition of MeI (1.3 g, 9.8 mmol) via syringe caused a rapid change to a yellow color. The reaction mixture was stirred for 10 min before the ice bath was removed, and stirring was continued for an additional 15 min. All volatile materials were removed under vacuum. The product was obtained as a white solid, after passage through a silica gel column using 1:1 hexanes/CH_2Cl_2 (2.12 g, 96%). X-ray-quality crystals were obtained by slow evaporation of a toluene solution of **1**. ^1H NMR (benzene-d_6, 300 MHz, 25 °C): δ 3.99 (q, 1H, C*H*), 2.35 (s, 6H, C*H*$_3$), 2.25 (s, 6H, C*H*$_3$), 2.18 (s, 6H, C*H*$_3$), 2.16 (s, 6H, C*H*$_3$), 1.35 (d, 3H, C*H*$_3$). $^{13}C\{^1H\}$ NMR (chloroform-*d*, 100 MHz, 25 °C): δ 146.0 (*C*), 138.5 (*C*), 134.5 (*C*), 133.4 (*C*), 128.4 (*C*), 127.9 (*C*), 42.0 (*C*H), 21.6 (*C*H$_3$), 18.9 (*C*H$_3$), 16.6 (*C*H$_3$), 16.4 (*C*H$_3$), 16.0 (*C*H$_3$). Anal. Calcd for $C_{21}H_{26}$: C, 90.35; H, 9.65. Found: C, 90.33; H, 9.77.

$Cp^*(C_{13}Me_8H)Ru$ (3). A THF solution (3 mL) of $LiCH_2SiMe_3$ (0.034 g, 0.36 mmol) was added to a THF solution (10 mL) of compound **1** (0.100 g, 0.36 mmol) at room temperature. The reaction turned a dark red and was stirred for 18 h. All volatile

(20) Connolly, J. W.; Urry, G. *Inorg. Chem.* **1963**, *2*, 645.
(21) Koelle, U.; Kossakowski, J. *Inorg. Synth.* **1992**, *29*, 225.
(22) Fagan, P. J.; Ward, M. D.; Calabrese, J. C. *J. Am. Chem. Soc.* **1989**, *111*, 1698.

materials were removed under vacuum. The resulting lithium derivative was suspended in benzene (8 mL), and a benzene solution (2 mL) of $[Cp^*RuCl]_4$ (0.085 g, 0.078 mmol) was added dropwise. The reaction mixture was stirred for 3 h, then all volatile materials were removed under vacuum. The product was extracted into toluene (ca. 5 mL), which was then filtered through a Celite plug, concentrated under vacuum, and cooled to −35 °C to yield the desired product as orange crystals (0.121 g, 75%). ^{1}H NMR (dichloromethane-d_2, 400 MHz, 25 °C): δ 5.18 (s, 1H, C*H*), 2.58 (s, 6H, CH_3), 2.26 (s, 6H, CH_3), 2.25 (s, 12H, CH_3), 1.24 (s, 15H, CH_3). ^{13}C{^{1}H} NMR (dichloromethane-d_2, 100 MHz, 25 °C): δ 128.6 (flu-*C*), 128.3 (flu-*C*), 127.9 (flu-*C*), 126.9 (flu-*C*), 97.7 (flu-*C*), 90.3 (flu-*C*), 80.75 (Cp*-*C*), 60.1 (flu-*C*H), 23.6 (flu-*C*H_3), 17.4 (flu-*C*H_3), 16.5 (flu-*C*H_3), 15.9 (flu-*C*H_3), 9.82 (Cp*-*C*H_3). Anal. Calcd for $C_{31}H_{40}Ru$: C, 72.48; H, 7.85. Found: C, 72.42; H, 7.84.

Cp*($C_{13}Me_9$)Ru (4). In a 20 mL vial, $LiMe_9Flu(THF)_{1.5}$ (0.100 g, 0.247 mmol) (preformed by the deprotonation of the ligand with $LiCH_2SiMe_3$ in THF followed by drying under vacuum; the stoichiometric ratio of THF was assessed by ^{1}H NMR after hydrolysis of a sample in benzene-d_6) was suspended in benzene (6 mL), and a benzene solution (2 mL) of $[Cp^*RuCl]_4$ (0.067 g, 0.062 mmol) was added dropwise. The reaction was stirred for 1 h, then all volatile materials were removed under vacuum. The solids were washed with hexanes (5 mL) and extracted with toluene (ca. 5 mL), and the extract was filtered, concentrated under vacuum, and cooled to −35 °C to yield the desired product as a yellow solid (0.061 g, 47%). X-ray-quality single crystals were grown from a hexanes solution cooled to −35 °C. ^{1}H NMR (dichloromethane-d_2, 300 MHz, 25 °C): δ 2.82 (s, 3H, CH_3), 2.47 (s, 6H, CH_3), 2.46 (s, 6H, CH_3), 2.24 (s, 6H, CH_3), 2.23 (s, 6H, CH_3), 1.26 (s, 15H, CH_3). ^{13}C{^{1}H} NMR (dichloromethane-d_2, 75 MHz, 25 °C): δ 129.6 (flu-*C*), 128.5 (flu-*C*), 128.2 (flu-*C*), 127.8 (flu-*C*), 97.1 (flu-*C*), 90.1 (flu-*C*), 81.0 (Cp*-*C*), 70.8 (flu-*C*), 23.6 (flu-*C*H_3), 18.3 (flu-*C*H_3), 17.6 (flu-*C*H_3), 17.4 (flu-*C*H_3), 16.8 (flu-*C*H_3), 9.4 (Cp*-*C*H_3). Anal. Calcd for $C_{32}H_{42}Ru$: C, 72.83; H, 8.02. Found: C, 72.96; H, 8.30.

Electrochemical Measurements. The electrochemical analyses were performed with use of a Bioanalytical Systems (BAS) Model CV-50W electrochemical analyzer. Cyclic voltammetry (CV) measurements were performed at room temperature (ca. 20 °C) with a normal three-electrode configuration consisting of a highly polished glassy-carbon-disk working electrode (A = 0.07 cm^2), a $Ag/AgNO_3$ reference electrode containing 0.1 M $TBA^+ClO_4^-$ in CH_3CN, and a platinum-wire counter electrode. The working component of the electrochemical cell was separated from the reference compartment by a porous Vycor tip. Analyses were performed on 5.0−7.5 mL of ca. 0.5 mM solutions of the organometallic complexes. The dichloromethane solvent used for all electrochemical experiments was distilled from CaH_2 under an atmosphere of nitrogen. $TBA^+ClO_4^-$ was purchased from Fluka. The working solutions were prepared in a glovebox (VAC) and syringed into a cell under a nitrogen counter flow. The redox potentials of the transition-metal complexes were calibrated with the ferrocenium/ferrocene (Fc^+/Fc) couple, which was defined at 0.47 V and was determined before and after each series of runs. Several measurements were repeated with ferrocene as an internal standard to verify the accuracy of the measurements.

Table 3. Selected Crystal Data and Data Collection Parameters for 1, 2, and 4

	1	**2**	**4**
formula	$C_{21}H_{26}$	$C_{22}H_{28}$	$C_{32}H_{42}Ru$
fw	278.42	292.44	527.73
T (K)	136(2)	157(2)	127(2)
wavelength (Å)	0.71073	0.71073	0.71073
cryst syst	orthorhombic	monoclinic	monoclinic
space group	*Pccn*	*C*2/*c*	*Cc*
a (Å)	17.4698(8)	23.89(2)	11.262(3)
b (Å)	24.6082(11)	9.191(9)	31.713(10)
c (Å)	7.3072(3)	15.890(14)	7.774(2)
α (deg)	90	90	90
β (deg)	90	101.06(2)	113.492(4)
γ (deg)	90	90	90
V (Å^3)	3141.4(2)	3424(5)	2546.4(13)
Z	8	8	4
abs coeff (mm^{-1})	0.066	0.063	0.634
final R indices	0.0388	0.0762	0.0343
	0.0985	0.2175	0.0876

Crystallographic Structure Determinations. Crystallographic data for all compounds are summarized in Table 3. All crystals were mounted on a glass fiber using Paratone-N oil. The Laue symmetry of each was photographically determined, and the space groups were assigned unambiguously for **1**, **2**, and **4** from systematic absences. All structures were solved by direct methods, refined with anisotropic thermal parameters, and include idealized hydrogen atom contributions, except for **1**, where hydrogen atoms were located. All computations were performed using SHELXTL software (version 5.1, G. Sheldrick, Bruker Analytical X-ray Systems, Madison, WI.).

Acknowledgment is made to Dr. Fred Hollander, Dr. Allen Oliver, Jennifer McBee, and Joe Escalada for assistance with the X-ray crystallography. We thank Prof. Dermott O'Hare for sharing results on an alternative synthesis of $C_{13}Me_9H$, prior to publication. This work was supported by the Director, Office of Energy Research, Office of Basic Energy Sciences, Chemical Sciences Division, of the U.S. Department of Energy under Contract No. DE-AC02-05CH11231, and P.B. thanks NSERC for a postdoctoral fellowship.

Supporting Information Available: Crystallographic data (tables and CIF files) for **1**, **2**, and **4** are available free of charge via the Internet at http://pubs.acs.org.

OM0603464